

11  
1437  
c.1

**NASA**  
**Technical Paper 1437**

**AVRADCOM**  
**Technical Report 78-42**

LOAN COPY: RETURN  
AFWL TECHNICAL LIBRARY  
KIRTLAND AFB, N. M.



# Thermal Stress Analysis of Ceramic Gas-Path Seal Components for Aircraft Turbines

**Francis E. Kennedy and Robert C. Bill**

**APRIL 1979**





NASA

Technical Paper 1437

Technical Report 78-42

# Thermal Stress Analysis of Ceramic Gas-Path Seal Components for Aircraft Turbines

Francis E. Kennedy  
*Lewis Research Center  
Cleveland, Ohio*

and

Robert C. Bill  
*Propulsion Laboratory, AVRADCOM Research and Technology Laboratories  
Lewis Research Center  
Cleveland, Ohio*



National Aeronautics  
and Space Administration

**Scientific and Technical  
Information Office**

1979

## SUMMARY

Stress and temperature distributions were evaluated numerically for a blade-tip seal system proposed for gas turbine applications. The seal consists of an abradable ceramic layer on a metallic backing with intermediate layers between the ceramic layer and metal substrate. The most severe stresses in the seal, as far as failure is concerned, are tensile stresses at the top of the ceramic layer and shear and normal stresses at the layer interface. All these stresses reach their maximum values during the deceleration phase of a severe engine test cycle.

A parametric study was carried out to evaluate the influence of various material and geometric parameters on these critical stress values. It was found beneficial to use a backing material with low modulus, high thermal conductivity, low thermal expansion, and low heat capacity. Studies of the ceramic layer showed that a layer of reduced density (or increased porosity) and lower modulus and thermal conductivity would be subject to reduced stresses. An investigation of the intermediate layers shows that it is beneficial to have a low modulus, high conductivity material between the ceramic layer and metallic substrate.

After the parametric study was completed, a seal system was designed which incorporated materials with the desirable elastic and thermal properties in each layer of the seal. An analysis of the proposed seal design showed an appreciable decrease (62.5 percent) in the magnitude of the maximum critical stresses over those obtained with earlier configurations.

## INTRODUCTION

Continuing attempts to develop more efficient and economical aircraft gas turbines require improved designs of engine components. One very important component, from the standpoint of engine performance, is the outer gas-path seal in the high-pressure turbine section of the engine, an example of which is shown in figure 1. Turbine gas-path seals perform two primary functions: (1) maintain minimum clearance over the rotating blade tips, thereby reducing aerodynamic and leakage losses, and (2) provide a thermal barrier between the hot turbine gases and the stationary turbine structure, thereby protecting critical turbine parts from excessive temperatures.

The efficiency of a gas turbine engine can be increased significantly by reducing the tip clearance of the gas-path seals (ref. 1). Reduced tip seal clearances limit the leak-

age of high-pressure gas from the turbine before useful work can be extracted from it. Such reductions in clearance may, however, result in occasional rubbing between the seal and the rotating blade tips as differential thermal expansion and engine deflections occur. To insure that the blade-tip seal rubs do not cause significant wear of the metallic blades and to minimize the effect of rubs on tip seal clearance, the surface of the seal should be abradable so that it wears preferentially during blade tip - seal interactions.

The inlet gas temperatures in modern high-pressure turbines frequently exceed 1589 K (2400<sup>o</sup> F), and these temperatures will be increasing in the next few years to improve turbine efficiency. Since present-day metallic seal systems are limited to about 1366 K (2000<sup>o</sup> F), cooling air must be bled from the compressor section and used to maintain the seal components within material operating capabilities. This condition results in a loss of engine performance as high-pressure air is removed from the cycle; such losses would increase if higher turbine inlet temperatures necessitated greater cooling. Substantial benefits would arise if materials with a high temperature capability were employed in the outer gas-path seals of high-pressure turbines. Additional benefits could be obtained if the materials of the seal surface had a low thermal conductivity; with a low-thermal conductivity the engine's structural components would be insulated from high temperatures and the need for cooling the structural components would be limited.

One of the most promising gas-path seal systems which has been proposed to meet these requirements is a plasma-sprayed, multilayered yttria-stabilized zirconia-CoCrAlY system on a metallic substrate (ref. 2). The yttria-stabilized zirconia (YSZ) material is abradable and can accommodate turbine inlet temperatures of about 1810 K (2800<sup>o</sup> F) (ref. 3). Although this proposed ceramic material meets the abradability and temperature requirements for gas-path seal applications, its brittleness and low strength require that the YSZ layer be supported by a metal backing. Differences in thermal expansion between the YSZ ceramic and candidate metals are such that failure of the seal system by cracking or delamination of the ceramic is likely unless intermediate layers are employed between the YSZ layer and the metallic backing. A graded series of ZrO<sub>2</sub> - CoCrAlY intermediate layers has been proposed to overcome this problem (ref. 2); however, the resulting seal system does not seem to have sufficient thermal shock or fatigue resistance to withstand prolonged use in an actual engine. Implementing design changes to alleviate this problem requires a better understanding of the expected stress distribution in a ceramic seal system and of the parameter which affect such stresses.

It was the objective of this research to study the stresses and temperatures in a ceramic gas-path seal during a severe-turbine test cycle and to determine the effect of various material and geometric parameters on those stresses and temperatures. Among the parameters to be investigated are the elastic and thermal properties of the

seal materials and the thicknesses of the various seal layers. The results of the parametric study will be used as a basis for design recommendations, the implementation of which should lead to better, longer lasting gas-path seals.

## ANALYTICAL PROCEDURES

The particular seal system studied in the analysis was the rotor tip seal of a test version of a high-pressure turbine for which relatively complete geometric and engine temperature data were available (ref. 2). The seal configuration is shown in figure 2. The outside dimensions of the seal were not changed during the study, but the thickness and composition of the surface layer, intermediate layers, and backing layers were varied.

The engine cycle under consideration was a severe test cycle consisting of acceleration, steady-state sea-level takeoff, deceleration, and idle. Since preliminary analyses of typical seal configurations showed that the most severe tensile stresses in the ceramic layer occurred during deceleration of the engine from sea-level takeoff to idle conditions, most of the analytical efforts concentrated on that portion of the engine cycle. The temperature of the gases impinging on the seal during that 1-minute period was assumed to vary with time in the manner shown in figure 3, which is an idealized deceleration transient for the test cycle.

Because of the complex seal geometry and nonuniform temperature boundary conditions, simple analytical models, such as a thermoelastic layered beam model, proved inadequate and a numerical analysis was necessary. The analytical foundations for such an investigation were laid by earlier work at the NASA Lewis Research Center (ref. 4). The numerical techniques developed in that uncoupled thermal and thermoelastic seal study were modified and used in this investigation. The transient temperature distribution in a given seal design was obtained using the SINDA (Systems Improved Numerical Differential Analyzer) finite-difference program. Boundary conditions for the thermal analysis included convective heat transfer from the hot turbine gases to the ceramic surface and from the cooling air to the back face (see fig. 1). Since previous two-dimensional studies (ref. 4) showed that reasonable changes in the magnitudes of the surface convection coefficients do not significantly influence the transient temperature distribution, a parametric study of convection coefficients was not attempted here.

The temperature distribution in the seal at a given time in the engine cycle, as determined by the thermal analysis, was used in a thermoelastic stress analysis based on the finite-element method. Two different finite-element models were used, a three-dimensional model employing 20-node curved isoparametric brick elements and a hybrid model which combined the results from axisymmetric and plane stress studies. Both of these models used quadrilateral elements. The three-dimensional case, which was

analyzed using the MARC finite-element code, modeled one quarter of the seal shown in figure 2 (the seal is symmetric about axial and circumferential center planes); the axisymmetric analysis modeled half of the circumferential plane shown in figure 2; and the plane stress analysis modeled half of the axial plane. The axisymmetric and plane stress models were studied using the FEATAGS finite-element code. For the purposes of this study, no attempt was made to tie seal displacements to deformation of the engine shroud, but a point at the center of the seal was constrained in the plane stress and three-dimensional models to prevent rigid body motions. No residual stresses were assumed to be present in the seal system.

Preliminary analyses of typical seal configurations were carried out on both finite-element models to study the effect of mesh geometry (e. g. , size and aspect ratio of elements) on the results. Optimum mesh sizes were chosen on the basis of these studies: a three-dimensional model with 510 nodes, an axisymmetric model with 243 nodes, and a plane stress model with 209 nodes. These models were used throughout the remainder of the study. Comparing the three-dimensional results with those of the hybrid (plane stress - axisymmetric) model showed that the hybrid model predicted trends in stress distribution qualitatively consistent with the results of the three-dimensional study. Because of the greater economy of the hybrid analysis, it was decided to use the hybrid model as a workhorse during most of the parametric study when trends in the results were of primary importance. The more accurate three-dimensional analysis was used to determine the stress magnitudes in seal configurations which implemented the recommendations of the parametric study. It was also used occasionally to check the trends determined with the hybrid model.

An additional set of preliminary studies was carried out to determine the magnitude and location of the most significant stresses in the seal, to relate these stresses to failure modes that have been observed in tests of prototype seal configurations (ref. 2), and to determine the time in the turbine cycle when the most critical stress magnitudes are reached. Two major failure modes have been determined in prototype seals: cracking of the top surface of the ceramic layer, due to the presence of axial and circumferential tensile stresses at the ceramic surface, and delamination of the ceramic layers, probably caused by radial and shear stresses at the interface between layers at the edge of the seal. Because of this, the stresses of most importance in this study were the axial and circumferential stress components at the top center of the ceramic layer and the radial and shear stresses near the interface between the layers at the outside edge of the seal.

An analysis of the stress and temperature distributions in typical seal configurations showed that each of the critical stress components reached its maximum value approximately 12 seconds into the cycle shown in figure 3. The reason for this is that at that time in the cycle the temperature on the seal surface is most significantly lower than the subsurface temperature because the impinging gas had cooled more rapidly than

had the bulk of the ceramic seal material. Earlier studies (ref. 4) also showed this phenomenon. Therefore, the most important stress values in the parametric study were those occurring 12 seconds into the cycle.

## RESULTS AND DISCUSSION

### Parametric Studies

Analyses were carried out using the previous procedures to study the effects of the various seal design parameters on the critical temperatures and stresses in the seal. Material properties were varied for each of the three sections of the seal, backing intermediate layers, and ceramic layer (see fig. 2). In each case the outside configuration of the seal was left unchanged. For each seal section, in addition to variations in individual material properties, practical material selection constraints were considered.

Backing material. - The influence of the properties of the metallic backing material on the stresses in the ceramic layer was studied. The baseline configuration, suggested by reference 2, included a 1.52-millimeter- (0.06-in. -) thick layer of yttria-stabilized zirconia (YSZ) ceramic and three graded YSZ-CoCrAlY intermediate layers. All the test configurations contained surface and intermediate layers of those same materials and dimensions. The backing material for the baseline configuration was Hastelloy X, and each of the other configurations had one material property different from the Hastelloy X properties. The material properties which were varied were coefficient of thermal expansion ( $\alpha$ ), modulus of elasticity (E), thermal conductivity (K), and heat capacity ( $\rho c$ ).

The results of the parametric study are shown in table I. It can be seen that it is desirable to choose a backing material with low heat capacity, low modulus, and high thermal conductivity. The thermal expansion of the backing material had a strong, but somewhat mixed, influence on the stresses in the ceramic with a given change in  $\alpha$  causing some stress components to increase and others to decrease. A backing material with low thermal expansion would probably be best under most circumstances.

Although the role of the backing material in the potential failure of the ceramic seal is an important design consideration, other considerations limit the choice of possible backing materials. Because of the high temperatures encountered by the backing, good high-temperature strength, creep resistance, and oxidation resistance are important requirements. Of the materials which meet these requirements none have all the properties that the parametric study found desirable. Two candidates which do appear interesting, mainly because of their high thermal conductivity (45 to 50 percent higher than Hastelloy X at 800 K), are the cast cobalt-based alloys WI-52 and MAR-M-509. Results for these materials are shown in table I, and it is seen that WI-52, in particular,

reduces considerably the stresses both at the top of the ceramic layer and at the layer interface.

Intermediate layers. - In an attempt to minimize the cracking and delamination of the ceramic layer due to thermal expansion differences between the ceramic and metallic backing materials, it is desirable that intermediate layers be employed between the ceramic layer and metal substrate. An earlier work (ref. 2) proposed using three plasma-sprayed cerametallic layers with the top layer (adjacent to the ceramic) being composed of 85-percent yttria-stabilized zirconia (YSZ) and 15-percent CoCrAlY alloy. The middle layer was 70-percent YSZ with 30-percent CoCrAlY, and the lowest layer (adjacent to the metal) was 40-percent YSZ with 60-percent CoCrAlY. These three intermediate layers, each 0.76 millimeter (0.03 in.) thick, were used in the baseline configuration for this comparative study with the baseline ceramic layer being 1.52-millimeter- (0.06-in. -) thick YSZ and the backing being MAR-M-509.

In order to study the effect of a variety of proposed intermediate layers, seven different configurations were investigated; these configurations are listed in table II. For each of the configurations the backing material was MAR-M-509 and the backing thickness was kept at 2.79 millimeters. Table II shows that several of the configurations involve different numbers and thicknesses of intermediate layers using the same materials as those in the baseline configuration. One configuration (no. 4) uses layer materials similar to those of the baseline except that the thermal conductivity of the intermediate layers is doubled. Configurations 5 to 7 employ a single intermediate layer composed of a porous metal with properties similar to 20-percent-dense Haynes 188, a cobalt-based alloy. Low-modulus, porous (or fiber) metal materials such as this have been used in compressor gas-path seal applications in recent years. The elastic modulus of 20-percent-dense, porous, metal materials can be about three orders of magnitude lower than solid, 100-percent-dense, materials of the same composition, while the material's thermal conductivity can be two orders of magnitude lower than the 100-percent-dense values.

From the results of the analysis, shown in table II, it can be seen that a thicker ceramic layer with two, instead of three, intermediate cerametallic layers (configuration 3) gives lower stresses at the ceramic surface than at the baseline, but the interlaminar shear stresses are increased. Increasing the conductivity of the intermediate layers decreases the surface stresses still further, but the interlaminar shear stresses are increased further. Thus, the possibility of seal failure due to the ceramic cracking would be lessened by using configurations 3 and 4, but delamination of the ceramic would be more likely.

Using a low-modulus, porous, metallic, intermediate layer results in much lower interlaminar shear stresses than when using the cerametallic layers, but the surface tensile stresses, at least those in the axial direction, are not as low as those with two high-conductivity cerametallic layers (configuration 4). Delamination could be effec-



tively eliminated by using a porous intermediate layer, although surface cracking would still exist. The reason for the surface stress problem can be seen from the temperature distribution shown in figure 4. The maximum temperature occurs well within the ceramic layer, and the resulting variation in thermal deformation causes tensile stresses at the top of the ceramic. The poor thermal conductivity of the porous layer contributes to this problem by limiting the transfer of heat from the ceramic to the backing.

Another practical problem with the porous metal layers is that the maximum temperatures in the porous metal, which occur under takeoff conditions, may exceed the maximum recommended use temperature (in air) for such materials. Although the material chosen for the study (Haynes 188) is one of the most oxidation resistant of the available porous metals, it can encounter severe oxidation and deterioration if the temperature gets much higher than 1150 K (ref. 5). As can be seen from figure 5, the maximum temperatures in the porous metal layers approach or exceed the critical values. The thinner porous metal layers, such as configuration 7, showed lower temperatures in the porous metal, but difficulty in bonding such thin layers without modifying their properties may restrict their use.

Since a major reason for the high temperatures and tensile stresses encountered with the porous layers is their poor ability to conduct heat away from the hot ceramic surface, an additional analysis was carried out to determine the effect of increasing the radial conductivity of the porous material by a factor of 5. Such an increase could be obtained by running wires or pins through the porous layer in the radial (thickness) direction to increase its density in the radial plane by about 20 percent. The results of that study are shown in figures 4 and 5 where it can be seen that the increased radial conductivity gives significantly improved temperature distributions. The maximum temperature in the porous layer could be reduced to within the temperature limitations of the material (fig. 5), and the temperature variation in the ceramic layer 12 seconds into the cycle (fig. 4) is much less severe. The stresses in the ceramic layer were considerably reduced at the 12-second interval; the maximum axial and circumferential tensile stresses were reduced 13 and 38 percent below their baseline values and the interlaminar shear stress was reduced 72 percent below its baseline. Since any of the procedures envisioned for increasing the radial conductivity would also increase substantially the stiffness in the radial direction, the stress analysis for this case assumed a radial elastic modulus of 50 times the normal value for the porous material. Consequently, the layer was assumed to have orthotropic thermal and elastic properties.

Ceramic layer. - Although the proposed yttria-stabilized zirconia ceramic seems to satisfy most of the requirements for the turbine gas-path seal surface, it was deemed desirable to study the influence of the ceramic's properties on the stresses in the ceramic and at the interface. The material properties of most interest are elastic modulus, thermal conductivity, and heat capacity. Each of these properties could be modified

by changing the density of the YSZ ceramic layer. Although thermal expansion of the ceramic would also influence the stress distribution, its influence was not studied because changes in its value would require specification of a completely different ceramic.

The results of the parametric study are shown in table III. It can be seen that a decrease in each of the properties would reduce the stresses responsible for failure of the ceramic seal, although the influence of heat capacity was somewhat mixed. Since a decrease in the density of the ceramic layer would result in a reduction in each of these properties ( $E$ ,  $K$ , and  $\rho c$ ), an additional configuration (no. 5) was studied in which all the properties were reduced simultaneously. The results for that case were quite encouraging (table III).

In order to investigate further the advantages of reducing the properties of the ceramic layer, two configurations which appear feasible were investigated. The first involved using a ceramic with 90-percent density (10-percent reduction from baseline density). It was estimated that such a decrease in density would result in approximately a 50-percent reduction in both elastic modulus and thermal conductivity while giving a 10-percent reduction in heat capacity. Since it appeared from the earlier results that it might be desirable to have a higher conductivity at the back of the ceramic layer (near the interface with the intermediate layer) than at the top surface, a configuration was analyzed which had a linear gradation in density (and, therefore, conductivity and modulus) from 90-percent of the baseline density at the top to 100 percent at the interface.

The results for these two configurations are shown in figures 6 to 8. In figure 6 the temperature distribution is compared with that obtained for other ceramic layer configurations. The graded ceramic is seen to give a slightly less severe temperature gradient near the surface than does the uniform low-density ceramic, and this results in slightly lower stresses at the ceramic surface (figs. 7 and 8). Both of these configurations give significantly lower tensile stresses at the top of the ceramic layer than were obtained with the baseline configuration. A decrease in the stresses at the layer interface was also noted with those two configurations, but the reductions were not as significant as were the tensile stress reductions shown in figures 7 and 8.

### Design Implications

The parametric studies showed that the critical tensile and shear stresses in a ceramic gas-path seal can be decreased if a metallic backing material is chosen which has low elastic modulus, high thermal conductivity, and low heat capacity. Because of the high temperatures encountered by the backing material and its strength and oxidation resistance requirements, the material choices for this application are limited and no single material combines all the desirable characteristics. Several cobalt-based alloys,

including WI-52 and MAR-M-509, appear to be suitable, however, mainly because of their reasonably high thermal conductivity.

Studies of the properties and geometry of the ceramic (yttria-stabilized zirconia) layer showed that a YSZ layer with reduced elastic modulus, density, and thermal conductivity would encounter lower stresses than would solid (100-percent dense) YSZ. Although a layer with graded density (low density at top surface, higher density at back interface) gave slightly better results than a uniform layer of reduced density, the uniform layer would be easier to produce. Such a reduction in density could probably be obtained by either spraying from a greater distance or by using a burnout technique in which some expendable powder (such as a polymer) would be included in the plasma spray. A reduction in density of only 10 percent was found to be effective in reducing stresses in the ceramic layer.

An investigation of the intermediate layers showed that it is desirable to have a low-modulus, high-conductivity material between the ceramic layer and the metallic backing. One possible way to achieve these properties would be to use an oxidation resistant, porous metal intermediate layer. Embedding pins or wire in the layer to improve its thermal conductivity in the radial direction would be very beneficial. Other alternatives include using two graded intermediate layers of YSZ-CoCrAlY, although delamination of the layers would be more likely to occur with such a system.

The combined results of the parametric studies show that an optimum ceramic seal system would have relatively flexible (low  $E$ ) materials in each layer. This would help limit the buildup of stress in the seal due to the nonuniform thermal strains encountered during operation. The optimum seal would also have low heat capacity in each layer, thus enabling more rapid cooling (more heat loss per unit volume) of the entire seal during deceleration. More rapid and more uniform cooling would help prevent the detrimental situation, shown in figures 4 and 6, where the subsurface temperature is higher than that at the surface. This gives rise to damaging tensile stresses on the surface. The specification of high thermal conductivity in the intermediate and backing layers also helps alleviate this condition by providing a better path for conducting heat away from the hot ceramic and toward the cooler back surface. On the other hand, the top ceramic layer should have lower conductivity so that the entire seal is better insulated from the hot turbine gases.

After completing the parametric study, a seal system was designed which incorporated materials having the characteristics suggested by the parametric studies in each layer of the seal. The seal backing material was WI-52, the intermediate layer was chosen to be a 1.52-millimeter-thick nickel-based porous metal with enhanced radial conductivity, and the 2.29-millimeter-thick yttria-stabilized zirconia ceramic layer had a uniform density of 90 percent of theoretical. An analysis of the stresses in this optimized seal design was carried out using the three-dimensional finite-element model; it showed a significant reduction in the critical stress magnitudes over those obtained with

a design proposed earlier (ref. 2). The maximum tensile stress at the top of the ceramic layer was reduced by 62.5 percent from the value obtained with the original design (baseline configuration of table I). Other tensile stresses in the ceramic layer were also reduced considerably. The presence of the low-modulus intermediate layer led to interlaminar shear and radial stresses that were well below original values and were so low ( $<2.5$  MPa) that delamination would be unlikely with such a system as long as the porous layer did not deteriorate or oxidize in service. The maximum temperature of the porous material during the cycle was about 1035 K; this is below the value at which appreciable oxidation would be expected.

Numerous other gas-path seal designs are possible which would incorporate the conclusions of the parametric study. It is felt that the life of such seals, or of the optimized seal design described previously, would be significantly longer than that of previously proposed configurations.

### SUMMARY OF RESULTS

Based on the analytical study performed, the following general statements can be made:

1. The thermal and thermoelastic analyses reported herein showed that significant tensile stresses can occur at the top of the abradable ceramic layer of a turbine gas-path seal, and that these stresses become most severe when the turbine engine is decelerating from takeoff to idle conditions. Interlaminar shear and normal stresses also become most severe at that time.

2. A series of analytical parametric studies showed that the tensile and interlaminar shear stresses can be reduced if (1) the backing material has low modulus, high thermal conductivity, low density, and, probably, low thermal expansion, (2) the intermediate layers have low modulus and high thermal conductivity, and (3) the abradable ceramic layer has low density, low modulus, and low thermal conductivity.

3. A seal system was analyzed which incorporated materials with beneficial elastic and thermal properties in each layer of the seal, and it showed a decrease of 62.5 percent in the magnitude of the maximum tensile stress over that obtained with earlier configurations. Interlaminar shear stresses were reduced to nearly zero.

Lewis Research Center,  
National Aeronautics and Space Administration,  
Cleveland, Ohio, November 7, 1978,  
505-04.

## REFERENCES

1. Glassman, A. J., ed.: Turbine Design and Application. Vol. 2. NASA SP-209, 1973, p. 125.
2. Shiembob, L. T.: Development of a Plasma Sprayed Ceramic Gas Path Seal for High Pressure Turbine Applications. (PWA-5521, Pratt and Whitney Aircraft; NASA Contract NAS3-19759.) NASA CR-135183, 1977.
3. Stecura, S.: Two-Layer Thermal Barrier Coating for High Temperature Components. Am. Ceram. Soc. Bull., vol. 56, no. 12, Dec. 1977, pp. 1082-1089.
4. Taylor, C. M.; and Bill, R. C.: Temperature Distributions and Thermal Stresses in a Graded Zirconia/Metal Gas Path Seal System for Aircraft Gas Turbine Engines. NASA TM-73818, 1978.
5. Jarvey, W. T.; and Erickson, A. R.: Development of Improved Abradable Gas Path Seal Materials. AFML-TR-78-101, 1978.

TABLE I. - EFFECT OF BACKING MATERIAL PROPERTIES ON STRESSES IN  
CERAMIC (YSZ) LAYER 12 SECONDS INTO DECELERATION

| Backing material <sup>a</sup>   | Stress at top center of ceramic, percent difference from baseline |                                  |                                  | Radial stress (tensile) at interface, percent difference from baseline |
|---|---|----------------------------------|----------------------------------|--|
|   | Axial axisymmetric, $\sigma_z$                                    | Circumferential, $\sigma_\theta$ |                                  |  |
|   |   | Axisymmetric                     | Plane stress                     |  |
| Baseline (Hastelloy X)  | -----<br>(30.2 MPa)   | -----<br>(53.1 MPa)              | -----<br>(26.0 MPa)              | -----<br>(16.2 MPa)  |
| $(\rho c)_{\text{backing}} = \frac{1}{2} (\rho c)_{\text{Hastelloy X}}$ | -11.5   | -14.0                            | -9.8                             | -25.7  |
| $K_{\text{backing}} = 2 K_{\text{Hastelloy X}}$                         | -26.2   | -12.6                            | -20.9                            | -48.7  |
| $E_{\text{backing}} = \frac{1}{2} E_{\text{Hastelloy X}}$               | -27.0   | -10.8                            | -23.5                            | -70.3  |
| $\alpha_{\text{backing}} = 2 \alpha_{\text{Hastelloy X}}$               | -162  | +348                             | +20.1                            | +300   |
| $\alpha_{\text{backing}} = \frac{1}{2} \alpha_{\text{Hastelloy X}}$     | +84.8   | -175                             | -12.0 to +5.9<br>(center) (edge) | -151   |
| MAR-M-509   | -5.3  | -14.2                            | -7.3                             | -19.1  |
| WI-52   | +3.2  | -43.4                            | -12.7                            | -51.6  |

<sup>a</sup>Each system had same dimensions as baseline and same ceramic (1.524-mm YSZ) and intermediate layers (0.762-mm 85/15, 0.762-mm 70/30, 0.762-mm 40/60). All properties of backing material not explicitly stated are those of Hastelloy X.

TABLE II. - INFLUENCE OF INTERMEDIATE LAYER CONFIGURATION ON STRESSES IN CERAMIC SEAL 12 SECONDS INTO DECELERATION, AS DETERMINED BY AXISYMMETRIC ANALYSIS

| Configuration | Description  | Normal (tensile) stresses at top center of ceramic layer, percent change from baseline configuration |                   | Shear stress at layer interface (outside edge of seal), percent change from baseline configuration |
|---------------|--|--|-------------------|--|
|               |  | Axial  | Circumferential   |  |
| 1             | Baseline: 1.524-mm YSZ, 3 intermediate layers 0.762 mm thick (85/15, 70/30, 40/60), MAR-M-509 backing  | ---<br>(28.5 MPa)  | ---<br>(45.5 MPa) | ---<br>(30.9 MPa)  |
| 2             | 2.286-mm YSZ with no intermediate layers, MAR-M-509 backing  | -24  | +4                | +51  |
| 3             | 2.286-mm YSZ with 2 intermediate layers 0.762 mm thick (85/15 and 40/60), MAR-M-509 backing  | -47  | -14               | +16  |
| 4             | 2.286-mm YSZ with 2 intermediate layers of higher conductivity 0.762-mm thick ( $K_{\text{layer1}} = 2K_{85/15}$ , $K_{\text{layer2}} = 2K_{40/60}$ ), MAR-M-509 backing | -98  | -16               | +59  |
| 5             | 1.524-mm YSZ with one porous layer 2.286 mm thick and properties approximating 20-percent-dense Haynes 188, MAR-M-509 backing  | -7   | -34               | -101   |
| 6             | 2.286-mm YSZ with porous layer 1.524 mm thick of 20 percent dense Haynes 188, MAR-M-509 backing  | +12  | -27               | -100   |
| 7             | 3.048-mm YSZ with porous layer 0.762 mm thick of 20 percent dense Haynes 188, MAR-M-509 backing  | +14  | -26               | -98  |

TABLE III. - EFFECT OF PROPERTIES OF CERAMIC LAYER ON CERAMIC LAYER STRESSES 12 SECONDS INTO DECELERATION AS DETERMINED BY AXISYMMETRIC ANALYSIS

[Backing, MAR-M-509; intermediate layers, 1.524-mm 85-percent YSZ/15-percent CoCrAlY and 1.524-mm 40-percent YSZ/60-percent CoCrAlY.]

| Config-uration | Material properties<br><br>(a)  | Tensile stress at top of ceramic layer, percent difference from base-line configuration |                  | Radial tensile stress at layer interface, percent difference from baseline con-figuration |
|----------------|---|---|------------------|---|
|                |   | Axial   | Circum-ferential |   |
| 1              | Baseline (YSZ)  | ---   | ---              | ---   |
| 2              | $E_{\text{ceramic}} = \frac{1}{2} E_{\text{YSZ}}$   | (15.1 MPa)  | (39.1 MPa)       | (20.1 MPa)  |
| <sup>b</sup> 3 | $K_{\text{ceramic}} = \frac{1}{2} K_{\text{YSZ}}$   | -35   | -48              | -35   |
| 4              | $(\rho c)_{\text{ceramic}} = \frac{1}{2} (\rho c)_{\text{YSZ}}$   | -28   | -25              | -64   |
| 5              | $E_{\text{ceramic}} = \frac{1}{2} E_{\text{YSZ}}$<br>$K_{\text{ceramic}} = \frac{1}{2} K_{\text{YSZ}}$<br>$(\rho c)_{\text{ceramic}} = \frac{1}{2} (\rho c)_{\text{YSZ}}$ | -59   | +11              | -26   |
|                |   | -80   | -50              | -29   |

<sup>a</sup>Dimensions and all properties not specifically mentioned are same as baseline 2.286-mm Y<sub>2</sub>O<sub>3</sub> stabilized ZrO<sub>2</sub> (YSZ) ceramic layer.

<sup>b</sup>Configuration 3 from table II.

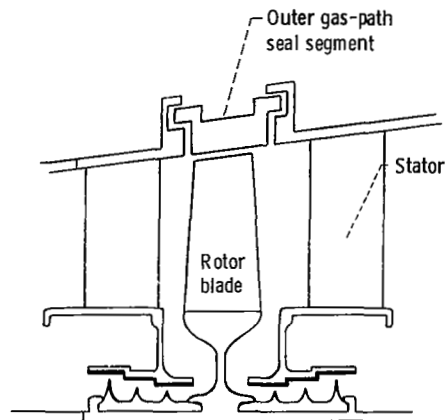
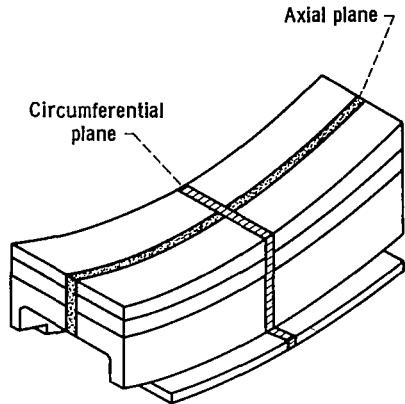


Figure 1. - High-pressure turbine outer gas-path seal.





Overall view

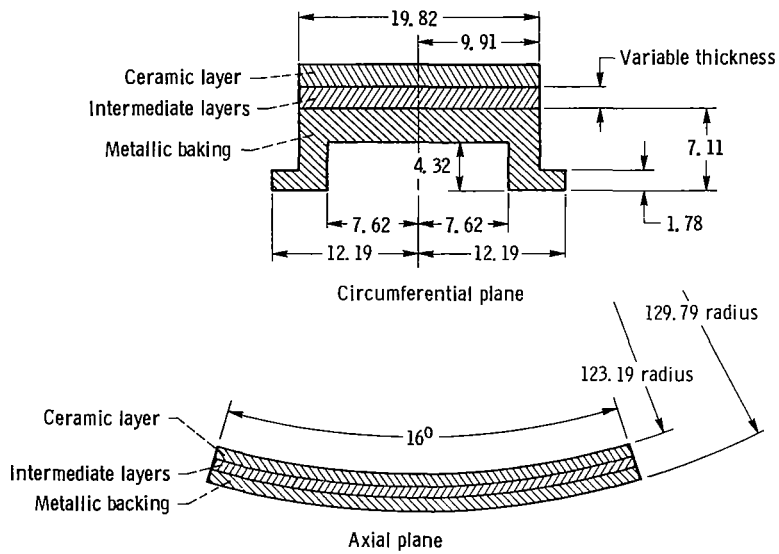


Figure 2 - Outer gas-path seal configuration. All dimensions are millimeters unless otherwise noted.

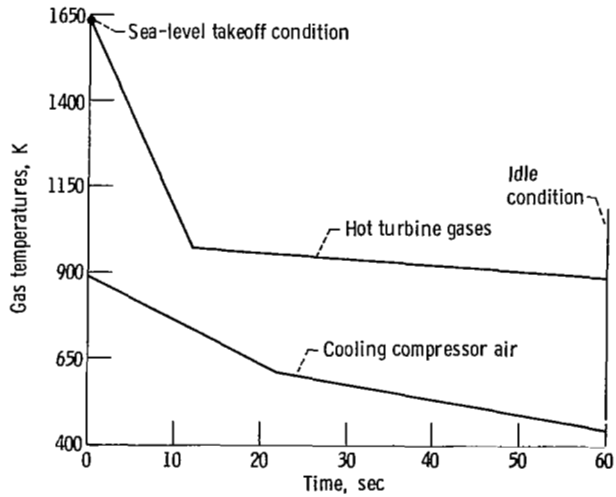


Figure 3. - Assumed gas temperature variations from sea-level takeoff to idle condition.

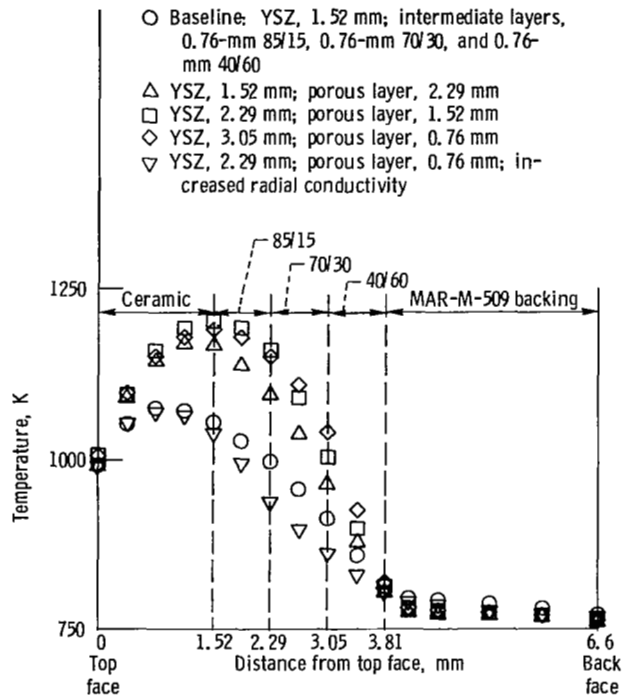


Figure 4. - Effect of intermediate layer configuration on temperature distribution along seal centerline 12 seconds into deceleration. MAR-M-509 backing.

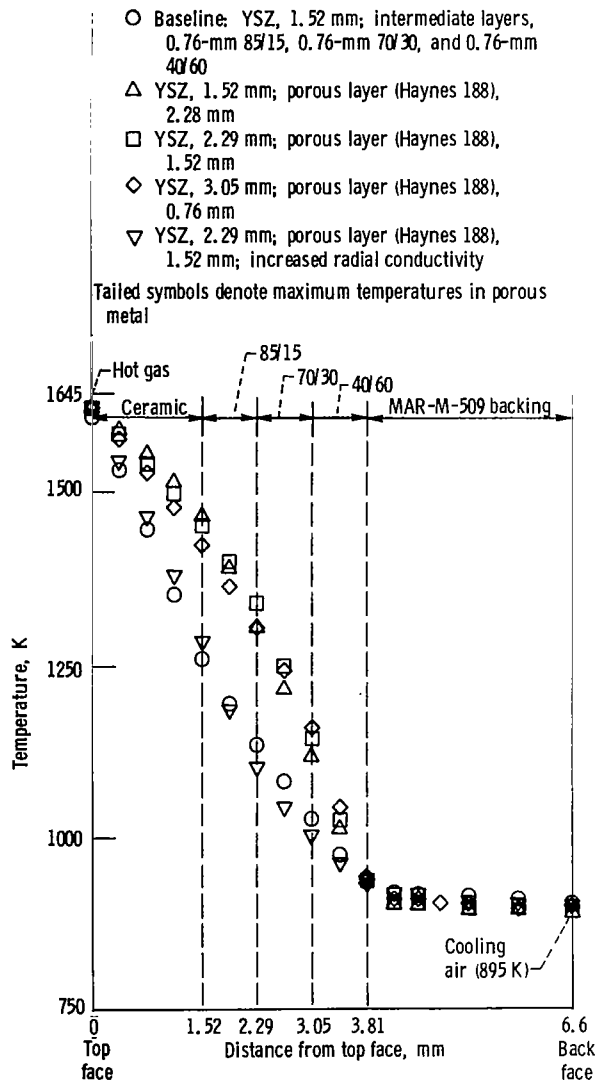


Figure 5. - Effect of intermediate layer configuration on temperature distribution along seal centerline at sea-level takeoff condition. MAR-M-509 backing.

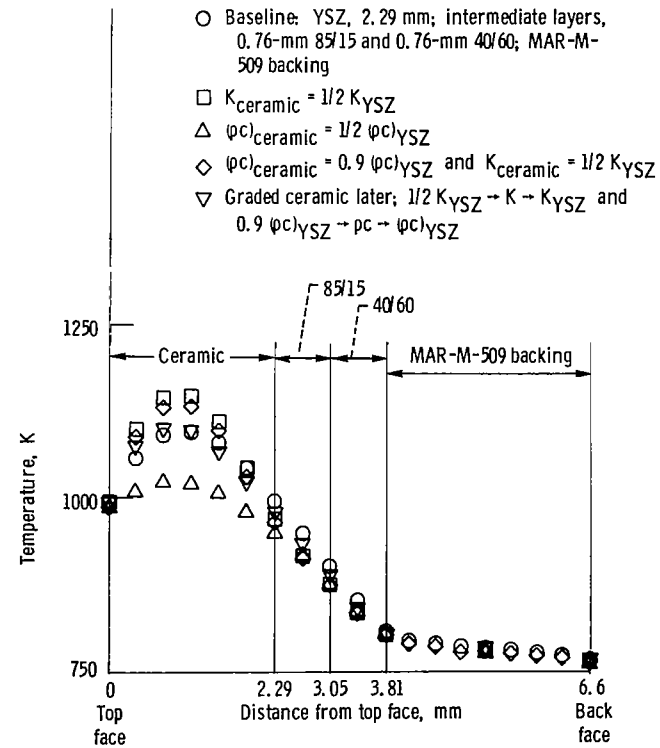


Figure 6. - Effect of ceramic properties on temperature distribution along seal centerline 12 seconds into deceleration.

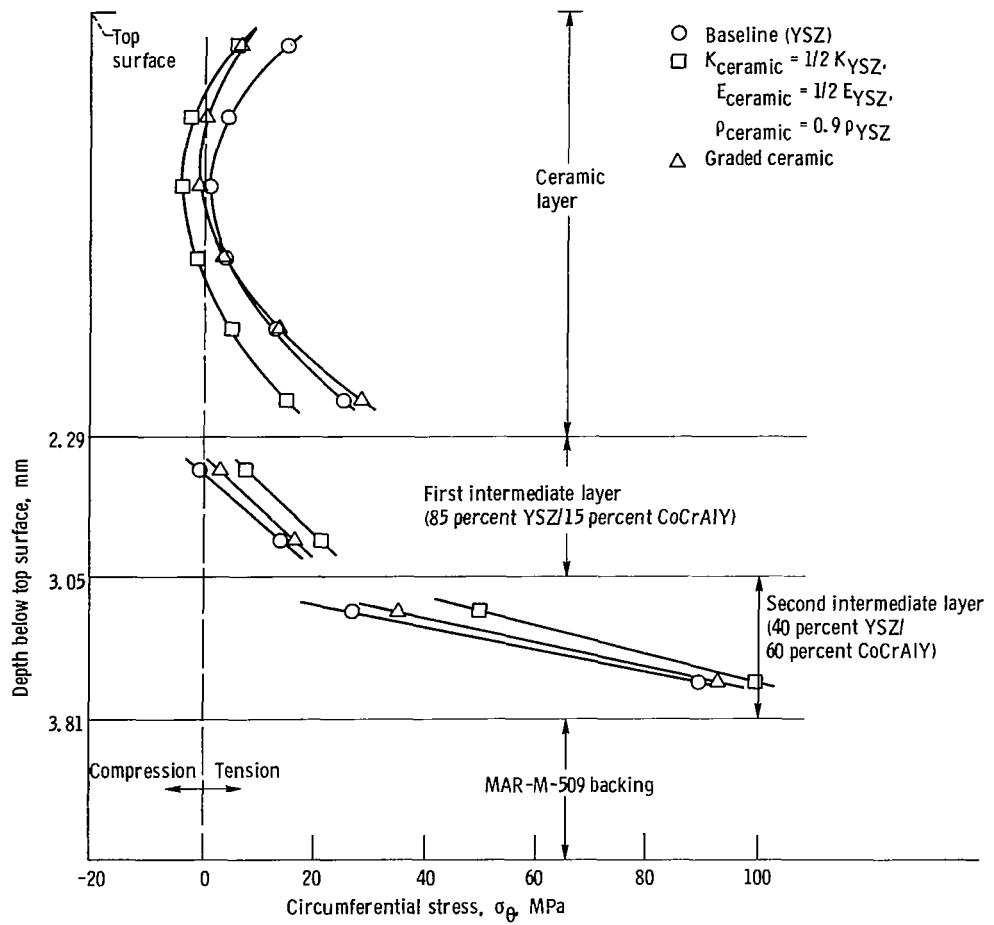


Figure 7. - Effect of ceramic properties on circumferential stress distribution along centerline of seal 12 seconds into deceleration. Plane stress analysis.

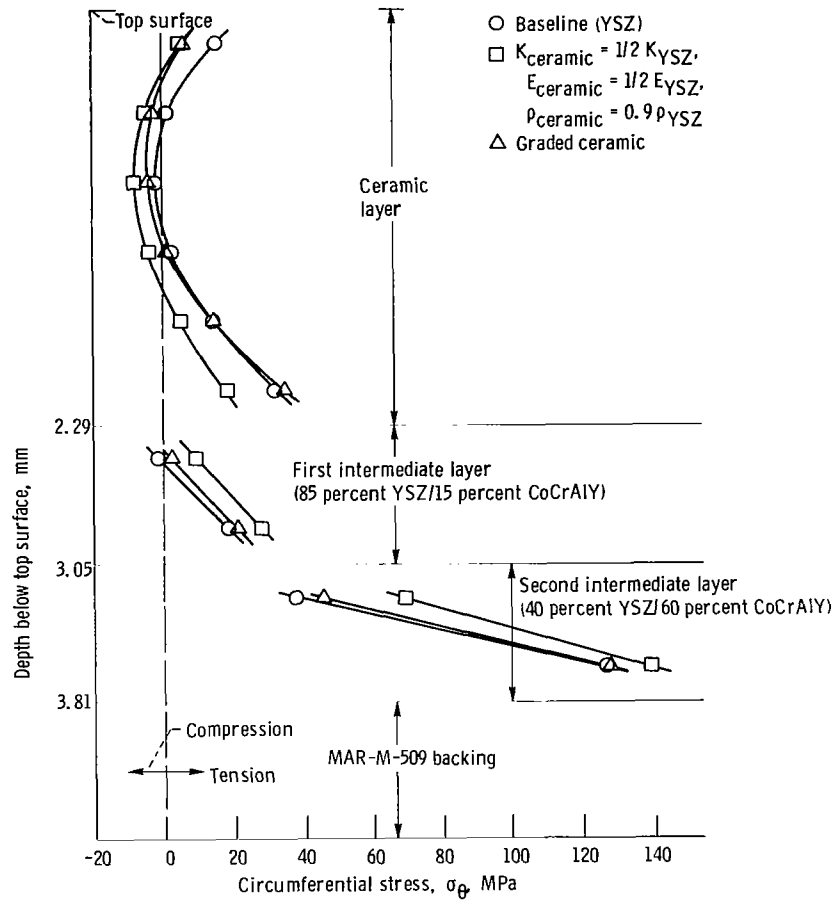


Figure 8. - Effect of ceramic properties on axial stress distribution along centerline of seal 12 seconds into deceleration. Axisymmetric analysis.

|  |  |  |  |  |                   |
|--|--|--|--|--|-------------------|
| 1. Report No. NASA TP-1437<br>AVRADCOM TR 78-42  |  | 2. Government Accession No.                          |  | 3. Recipient's Catalog No.                               |                   |
| 4. Title and Subtitle<br><b>THERMAL STRESS ANALYSIS OF CERAMIC GAS-PATH SEAL COMPONENTS FOR AIRCRAFT TURBINES</b>  |  |  |  | 5. Report Date<br>April 1979                             |                   |
|  |  |  |  | 6. Performing Organization Code                          |                   |
| 7. Author(s)<br>Francis E. Kennedy and Robert C. Bill  |  |  |  | 8. Performing Organization Report No.<br>E-9770          |                   |
| 9. Performing Organization Name and Address<br>NASA Lewis Research Center and<br>AVRADCOM Research and Technology Laboratories<br>Cleveland, Ohio 44135  |  |  |  | 10. Work Unit No.<br>505-04                              |                   |
|  |  |  |  | 11. Contract or Grant No.                                |                   |
| 12. Sponsoring Agency Name and Address<br>National Aeronautics and Space Administration<br>Washington, D.C. 20546 and U.S. Army Aviation Research and<br>Development Command, St. Louis, Mo. 63166   |  |  |  | 13. Type of Report and Period Covered<br>Technical Paper |                   |
|  |  |  |  | 14. Sponsoring Agency Code                               |                   |
| 15. Supplementary Notes<br>Francis E. Kennedy, Dartmouth College, Hanover, N. H., and Summer Faculty Fellow,<br>Lewis Research Center, 1977 and 1978; Robert C. Bill, AVRADCOM Research and<br>Technology Laboratories.  |  |  |  |  |                   |
| 16. Abstract<br>Stress and temperature distributions were evaluated numerically for a blade-tip seal system proposed for gas turbine applications. The seal consists of an abradable ceramic layer on a metallic backing with intermediate layers between the ceramic layer and metal substrate. The most severe stresses in the seal, as far as failure is concerned, are tensile stresses at the top of the ceramic layer and shear and normal stresses at the layer interfaces. All these stresses reach their maximum values during the deceleration phase of a test engine cycle. A parametric study was carried out to evaluate the influence of various design parameters on these critical stress values. The influences of material properties and geometric parameters of the ceramic, intermediate, and backing layers were investigated. After the parametric study was completed, a seal system was designed which incorporated materials with beneficial elastic and thermal properties in each layer of the seal. An analysis of the proposed seal design showed an appreciable decrease in the magnitude of the maximum critical stresses over those obtained with earlier configurations. |  |  |  |  |                   |
| 17. Key Words (Suggested by Author(s))<br>Thermal stress<br>Ceramic seal<br>Gas-path seal<br>Turbine seal  |  |  | 18. Distribution Statement<br>Unclassified - unlimited<br>STAR Category 27 |  |                   |
| 19. Security Classif. (of this report)<br>Unclassified   |  | 20. Security Classif. (of this page)<br>Unclassified |  | 21. No. of Pages<br>21                                   | 22. Price*<br>A02 |

\* For sale by the National Technical Information Service, Springfield, Virginia 22161

National Aeronautics and  
Space Administration

THIRD-CLASS BULK RATE

Postage and Fees Paid  
National Aeronautics and  
Space Administration  
NASA-451



Washington, D.C.  
20546

Official Business

Penalty for Private Use, \$300

16 1 10, C, 030979 S00903DS  
DEPT OF THE AIR FORCE  
AF WEAPONS LABORATORY  
ATTN: TECHNICAL LIBRARY (SUL)  
KIRTLAND AFB NM 87117

**NASA**

POSTMASTER:

If Undeliverable (Section 158  
Postal Manual) Do Not Return